AN INVESTIGATION OF TURNING OPERATION CHARACTERISTICS USING HYBRID NANOFLUID MINIMUM QUANTITY LUBRICATION (MQL)

A Synopsis submitted to Gujarat Technological University

for the Award of

Doctor of Philosophy

in

Mechanical Engineering

by

Mr. Nalbandh Altaf Hanifbhai

(Enrollment No.: 199999919525)

under supervision of

Dr. Neerajkumar K. Chavda

GUJARAT TECHNOLOGICAL UNIVERSITY

AHMEDABAD

May 2026

Table of Contents

AN INVESTIGATION OF TURNING OPERATION CHARACTERISTICS USING HYBRID NANOFLUID MINIMUM QUANTITY LUBRICATION (MQL)

Abstract

Turning is a fundamental machining operation in which a single-point cutting tool removes material from a rotating workpiece to generate cylindrical shapes, shoulders and grooves. Nanofluid-assisted minimum quantity lubrication (MQL) offers a promising route towards cleaner and more resource-efficient machining in line with UN Sustainable Development Goal 9, by reducing coolant consumption while maintaining or improving cutting performance. This thesis investigates the turning behaviour of AISI 1040 steel under thirteen cooling and lubrication conditions, including dry cutting, conventional wet cooling with water and SAE-40 oil, MQL with base oil, MQL with Al_2O_3 and ZnO mono nanofluids, and MQL with Al_2O_3–ZnO hybrid nanofluids prepared in SAE-40 oil. Cutting speed (31.71–107.55 m/min), feed (0.11–0.25 mm/rev) and depth of cut (0.2–0.6 mm) are varied according to a Box–Behnken Response Surface Methodology (RSM) design for each cooling condition, giving 195 experiments in total, from which cutting force, cutting temperature and surface roughness are measured. RSM models developed separately for all thirteen cases are statistically significant, with high coefficients of determination and satisfactory residual diagnostics confirmed by analysis of variance. Across conditions, feed and depth of cut are the dominant factors for all three responses, while cutting speed has a secondary but still meaningful effect. Comparative analysis of nanofluid formulations shows that Al_2O_3 favours lower forces and better surface integrity, whereas ZnO provides stronger temperature reduction; an intermediate nanoparticle concentration of 1 wt% gives the best overall balance. A desirability-based multi-response optimization (equal weighting, smaller-is-better) identifies MQL with 1 wt% Al_2O_3:ZnO (75:25, Case H1) as the most suitable overall lubrication condition among the thirteen cases and yields a global optimum at 107.55 m/min cutting speed, 0.11 mm/rev feed and 0.2 mm depth of cut. Validation tests at this setting show prediction errors of only 8.23% (force), 6.83% (temperature) and 3.56% (roughness), and reductions of about 25.1%, 18.26% and 16.33% in these responses, respectively, compared with dry cutting. In parallel, Artificial Neural Network modelling demonstrates that a feed-forward distributed time-delay network (N4P2T2) most accurately predicts the three responses across all cooling conditions, indicating that the combined RSM-desirability-ANN framework provides a robust, data-driven basis for designing sustainable, high-performance turning processes using hybrid nanofluid MQL.

A brief description of the state of the art of the research topic

In turning operation, the process performance is governed by cutting parameters, tool geometry, work material, and, critically, the conditions at the tool–workpiece interface, where high contact pressures and sliding velocities lead to severe frictional heating and mechanical loading that affect cutting forces, tool wear, chip morphology and surface integrity. Cutting fluids have long been used to mitigate these effects by cooling the cutting zone, lubricating the contact surfaces and flushing away chips, but conventional flood cooling with mineral or water-based emulsions requires large fluid volumes and is associated with high operating cost, environmental burden and health concerns for operators.

To address these issues, Minimum Quantity Lubrication (MQL) [1], [2], [3], [4] has emerged as a near-dry strategy in which a very small amount of lubricant-typically on the order of 10–100 ml/hr-is delivered as a fine aerosol directly to the cutting zone. Extensive experimental work shows that MQL can match or even surpass wet cooling in terms of cutting force, cutting temperature, tool wear and surface finish, while drastically reducing fluid consumption and disposal requirements and improving occupational hygiene. In parallel, nanofluids-formed by dispersing nanoscale particles of metals, metal oxides, carbides, nitrides or carbonaceous materials in a base fluid [5]-have been introduced to tailor the thermo-physical and tribological properties of cutting fluids. Under MQL, mono nanofluids based on Al_2O_3, SiO_2, TiO_2, CuO, MoS_2, graphite, graphene and carbon nanotubes [6], [7] have consistently been reported to lower cutting forces and temperatures, enhance tool life and improve surface roughness compared with conventional fluids, owing to enhanced thermal conductivity, formation of protective tribofilms and rolling or shear-reducing effects of the particles at the interface.

More recently, hybrid nanofluids that combine two or more nanoparticle types (e.g. Al_2O_3-MoS_2, Al_2O_3-graphene, Al_2O_3-TiO_2, Cu-Zn or multi-component mixtures [8]) have been proposed to exploit synergistic improvements in heat transfer and lubrication. Studies in turning indicate that such hybrid nanofluid MQL systems can further reduce friction and wear, increase allowable cutting speeds, decrease cutting temperature and energy consumption, and yield finer surface finishes than mono nanofluid MQL and conventional cooling. However, most reported work concentrates on specific work materials and limited ranges of cutting conditions, and relatively few studies integrate systematic designs of experiments, multi-response statistical optimization and ANN-based prediction within a single framework-particularly for medium-carbon steels like AISI 1040 and for oxide-oxide hybrid systems such as Al_2O_3-ZnO.

Definition of the Problem

The existing MQL turning literature on conventional and mono nanofluids still leaves key gaps for medium-carbon steels such as AISI 1040. In particular, Al_2O_3-ZnO hybrid nanofluids have not been systematically evaluated under MQL across multiple mixing ratios and concentrations while jointly modelling cutting force, cutting temperature and surface roughness, and most studies compare only one or two cooling strategies, limiting clear selection among dry, wet, mono-nanofluid MQL and hybrid-nanofluid MQL. Moreover, there is a lack of unified frameworks that combine statistically designed experiments, RSM, ANOVA, multi-response desirability optimization and ANN-based prediction to capture the strong nonlinear and interaction effects among cutting parameters, cooling conditions and nanofluid composition. This motivates a focused study that fills these gaps and quantitatively establishes the benefits of Al_2O_3-ZnO hybrid nanofluid MQL for turning AISI 1040 steel.

Objective and Scope of work

The turning process is a subtractive machining operation where a workpiece spins on a lathe while a stationary cutting tool moves linearly to shave away excess material. In this process, heat is generated as mechanical energy is transformed into thermal energy due to plastic deformation and friction. In conventional turning, cutting fluids are commonly used to reduce heat generation, lower friction, and improve surface quality. The flood-cooling constraints could be circumvented by replacing the cutting fluid with wet machining. MQL has emerged as a promising near-dry machining approach for reducing fluid usage while maintaining acceptable cooling and lubrication at the cutting zone. As a new class of cooling methods, Nanofluids with MQL are proposed and developed over the past decade for better heat transfer and excellent lubricating applications in turning.

Research Objectives

Following are the objectives of the present research work:

1. To experimentally investigate the effects of cutting speed, feed and depth of cut on turning performance under different cooling strategies (dry, wet, simple MQL, MQL with mono nanofluid and MQL with hybrid nanofluid).

2. To compare dry, wet, MQL+wet, MQL+mono nanofluid and MQL+hybrid nanofluid conditions in terms of cutting temperature, cutting force and surface roughness.

3. To determine the optimum cutting-fluid strategy and operating parameters for MQL-assisted turning, using multi-response optimization based on the measured performance indicators.

4. To develop and train Artificial Neural Network (ANN) models and identify the most accurate ANN architecture for predicting turning performance under different cooling conditions.

Scope of work

The following extent of research can be drawn from the study:

1. Use of Al_2O_3 and ZnO mono nanofluids and Al_2O_3-ZnO hybrid nanofluids to enhance the thermo-tribological performance of MQL during turning of AISI 1040 steel.

2. Preparation of stable and well-dispersed mono and hybrid nanofluids using a standardized

two-step process (weighing, magnetic stirring and ultrasonication) with SAE-40 oil as the base fluid.

3. Investigation of the effects of key parameters-nanoparticle concentration (0-2 wt%), Al_2O_3:ZnO mixing ratio in hybrid nanofluids, cutting speed, feed and depth of cut-on cutting force, cutting temperature and surface roughness under MQL.

4. Comparative study of dry cutting, wet cooling, mono-nanofluid MQL and hybrid-nanofluid MQL to identify lubrication conditions that most effectively improve machinability and surface integrity for AISI 1040 steel.

5. Identification of the optimum cutting-fluid strategy that delivers the best combined improvement in cutting force, cutting temperature and surface roughness under MQL turning of AISI 1040 steel.

6. Development of Artificial Neural Network (ANN) models to predict cutting force, cutting temperature and surface roughness from cooling condition, nanofluid composition and cutting parameters, thereby capturing the complex and nonlinear performance trends of nanofluid-assisted MQL turning.

Original contribution by the thesis

The outcome of the current research delivers a statistically designed experimental programme that compares thirteen cooling strategies-dry cutting, wet cooling, MQL with base oil, mono nanofluids and Al_2O_3-ZnO hybrid nanofluids-for turning AISI 1040 steel under identical cutting conditions, including a systematic evaluation of Al_2O_3-ZnO hybrids at three mixing ratios (25:75, 50:50, 75:25) and two nanoparticle loadings (1 wt% and 2 wt%). It develops and validates robust RSM models for cutting force, cutting temperature and surface roughness for each cooling condition using ANOVA, lack-of-fit tests and diagnostic plots, and implements a desirability-based multi-response optimization framework that ranks all strategies and clearly identifies 75:25 Al_2O_3:ZnO hybrid nanofluid MQL as the most effective option for jointly reducing force and temperature while maintaining acceptable surface finish. In parallel, it designs and evaluates a comprehensive set of ANN architectures yielding highly accurate predictive models for all three responses, which is a more expensive and time-consuming process.

The thesis of this research contains a brief discussion on turning, cutting fluid, MQL, its history, nanofluids and hybrid nanofluids, its preparation, artificial neural network technique under the heading of "Introduction." The discussion under the heading of "Review of the Literature" contains a study of MQL with conventional cutting fluids, with mono nanofluids and with hybrid nanofluids, statistical analysis, the motivation behind the research, Scope, and research objectives. Experimental setup preparation, nanofluid preparation, and design of experiments, RSM based Box-Behnken method with factors and responses, variables for ANN architecture, and errors calculation for performance prediction have been discussed under the heading of "Experimental Setup, Design of Experiments and Artificial Neural Network." Methodology for design of experiments and ANN are discussed under the heading of "Research Methodology." Comparison of cooling conditions in terms of output parameters had been discussed under the "Result and Discussion" section heading. The process of determine optimum cutting-fluid strategy using multi-response optimization had also been discussed in this section. The conclusion of the entire research work and physical justification and further expansion of this research have been discussed under the "Conclusion and Future scope" heading.

Methodology of Research, Results / Comparisons

Research Methodology

This entire research work has been divided into two parts (i) experimentation and (ii) development of ANN models. The experimental work subparts are nanofluid preparation and identification of cooling cases, experimental setup preparation, and DoE using RSM based Box-Behnken method. The ANN model's development has been carried out by creating, training, and simulating various ANN models for performance prediction of cooling conditions.

Nanofluid preparation and identification of cooling cases

Two different nano additives, Al_2O_3 and ZnO, were used in the present experimental investigation. All nanoparticles had been purchased from Platonic Nanotech Private Limited, Jharkhand, India. In the present experimental study, a two-step method was adopted for the nanofluids preparation. The nanoparticle Al_2O_3 and ZnO, with an average size range of 30-50 nm [9], [10] is employed to provide meaningful enhancement in thermal conductivity while limiting agglomeration, thereby maintaining good dispersion stability and sprayability in the MQL aerosol [11]. The nanoparticle concentration range of 1-2 wt% is selected in line with reported nanofluid-MQL studies [12], which show that very low loadings (< 0.5 wt%) yield only modest improvements, whereas higher concentrations above about 1.5-2 wt% [13] markedly increase viscosity, promote nozzle clogging, hinder atomization and can deteriorate surface finish and cutting forces [12], [14], [15]. The weighted mixer was then stirred for 2 hours using a magnetic stirrer and sonicated for 2 hours using an ultrasonic homogenizer to get stable and uniform nanofluids. Thirteen different cooling cases for dry, wet, MQL+wet wet, MQL+mono nanofluid and MQL+hybrid nanofluid have been prepared as shown in Table 1.

Table 1 Different cooling cases selected for experimentation

Case	Case Details
Case-A	Dry
Case-B	Wet conventional cutting fluid
Case-C	Wet SAE40 cutting fluid
Case-D1	MQL + 1% wt Al_2O_3
Case-D2	MQL + 2% wt Al_2O_3
Case-E1	MQL + 1% wt ZnO
Case-E2	MQL + 2% wt ZnO
Case-F1	MQL + 1% wt (Al_2O_3 : ZnO, 25:75)
Case-F2	MQL + 2% wt (Al_2O_3 : ZnO, 25:75)
Case-G1	MQL + 1% wt (Al_2O_3 : ZnO, 50:50)
Case-G2	MQL + 2% wt (Al_2O_3 : ZnO, 50:50)
Case-H1	MQL + 1% wt (Al_2O_3 : ZnO, 75:25)
Case-H2	MQL + 2% wt (Al_2O_3 : ZnO, 75:25)

Design of Experiments using RSM based Box-Behnken method

This study employs Response Surface Methodology (RSM) with a Box–Behnken Design (BBD) to examine the effects of three input variables-cutting speed, feed rate and depth of cut- on cutting force, cutting temperature and surface roughness during all thirteen cooling cases in turning of AISI 1040 steel. Cutting speed is varied at 31.71, 69.63 and 107.55 m/min, feed at 0.11, 0.18 and 0.25 mm/rev, and depth of cut at 0.2, 0.4 and 0.6 mm, with the selected ranges chosen to represent practical and stable machining conditions. The Box–Behnken design is adopted instead of Central Composite Design because it is more efficient for three-factor optimization and avoids extreme corner points that are difficult or unsafe to realize in turning experiments. For three factors at three levels, the BBD requires 15 experimental runs (12 edge points and 3 centre points) listed in Table 2, and the run order is fully randomized to minimise systematic bias; repeated centre runs provide an estimate of pure error, enabling a Lack-of-Fit test in the ANOVA based on the coded factor levels listed in Table 3.

Table 2 Box–Behnken Design Experimental runs

Test Run	**Cutting Speed (m/min)**	**Feed (mm/rev)**	**Depth of Cut (mm)**
1	69.63	0.25	0.2
2	69.63	0.11	0.6
3	31.71	0.18	0.6
4	107.55	0.18	0.2
5	107.55	0.25	0.4
6	69.63	0.25	0.6
7	107.55	0.11	0.4
8	69.63	0.18	0.4
9	69.63	0.18	0.4
10	69.63	0.18	0.4
11	31.71	0.11	0.4
12	31.71	0.25	0.4
13	31.71	0.18	0.2
14	107.55	0.18	0.6
15	69.63	0.11	0.2

Table 3 RSM Box Behnken Method input parameters with their coded factor levels

Input parameters	**Low (-1)**	**Center (0)**	**High (1)**
Cutting Speed (m/min)	31.71	69.63	107.55
Feed (mm/rev)	0.11	0.18	0.25
Depth of Cut (mm)	0.2	0.4	0.6

Experimental Setup

The performance of turning parameters for different cooling cases, was carried out using the experimental setup shown in Figure 1. The experimental setup for this study was prepared on a centre lathe (Banka 35–750 geared type) for straight turning of AISI 1040 steel bars of 50 mm diameter and 300 mm length. An external MQL system was integrated, comprising an SAE-40 oil reservoir, compressed-air supply, air–oil mixing chamber, pressure-control valve and a 2 mm nozzle delivering nanofluid at 360 ml/h and 3 bar towards the tool–chip interface. Deskar TNMG160408 CQ LF9218 carbide inserts were mounted in a tool holder, and cutting speed (31.71, 69.63, 107.55 m/min), feed (0.11, 0.18, 0.25 mm/rev) and depth of cut (0.2, 0.4, 0.6 mm) were set according to the Box–Behnken design matrix. Cutting force was measured using a strain-gauge dynamometer, cutting temperature with a Fluke 62 Max infrared thermometer, and surface roughness with a Mitutoyo SJ-210 portable tester, after which the setup was verified by trial runs under dry and wet conditions before nanofluid experiments.

Figure 1 Experimental setup along with MQL system

Procedure

The integrated research methodology adopted for performance evaluation is described below:

1. Prepare the nanofluid as mentioned in subsection of nanofluid preparation and identification of cooling cases by calculating the required mass of Al_2O_3 and ZnO for 1 and 2 wt% concentrations for each of the thirteen cases (A–H2) using the 120 ml volume of base oil.
2. Fill the external MQL reservoir with the prepared nanofluid, connect the compressed-air line and set the pressure-control valve to 3 bar. Adjust the nozzle (2 mm diameter) to direct the aerosol jet precisely at the tool–chip interface and fix the nanofluid discharge rate to 360 ml/h.
3. Start the spindle and feed, activate the chosen cooling condition (dry, wet, MQL with base oil, mono nanofluid or hybrid nanofluid), and perform a single straight turning pass for each design point.
4. Carry out, experiment for active cooling case, select the cutting speed (31.71, 69.63 or 107.55 m/min), feed (0.11, 0.18 or 0.25 mm/rev) and depth of cut (0.2, 0.4 or 0.6 mm) according to the corresponding BBD run.

5. Measure and record the three-output response cutting force (F), cutting temperature (T) at a fixed position with the IR thermometer during cutting, and surface roughness (Ra) along the machined surface using the SJ-210.
6. Clean the tool, workpiece surface and MQL lines when changing from one cooling condition to another to avoid cross-contamination.
7. Repeat Steps 1-6 for all 15 Box–Behnken runs in each cooling case (A–H2), generating a total of 195 experimental data sets.

Artificial Neural Network (ANN)

Different ANN models were trained using the full experimental dataset obtained from the thirteen cooling conditions. Of the total 195 data points, 80% were randomly selected for training and 20% reserved for testing, and prediction performance was evaluated for the errors in prediction in term of MSE (Mean Square Error), NMSE (Normalized Mean Square Error), MAE (Mean Absolute Error), and MARD (Mean Absolute Error). In total, 190 ANN architectures (as shown in Table 4) were created, trained and simulated in MATLAB 2014a, with cutting condition, Al_2O_3 proportion, ZnO proportion, cutting speed, feed and depth of cut as input parameters and cutting force, cutting temperature and surface roughness as target outputs. The best ANN model was proposed based on simultaneously achieving low prediction errors and a high coefficient of determination (R^2).

Table 4 Various ANN architectures

Neural Network	Performance function	Transfer function	No. of neurons at hidden layer	Model
Feed-forward backprop	MSE	TRANSIG	5 to 50 (in a gap of 5)	N1P1T1 to N1P1T10
Cascade-forward backprop	MSE	TRANSIG	5 to 50 (in a gap of 5)	N2P1T1 to N2P1T10
Elman-backprop	MSE	TRANSIG	5 to 50 (in a gap of 5)	N3P1T1 to N3P1T10
Feed-forward distributed time delay	MSE	TRANSIG	5 to 50 (in a gap of 5)	N4P1T1 to N4P1T10
Generalized regression	MSE	TRANSIG	Spread constant 1 to 5	N5P1T1 to N5P1T5
Feed-forward backprop	SSE	TRANSIG	5 to 50 (in a gap of 5)	N1P2T1 to N1P2T10
Cascade-forward backprop	SSE	TRANSIG	5 to 50 (in a gap of 5)	N2P2T1 to N2P2T10
Elman-backprop	MSE	TRANSIG	5 to 50 (in a gap of 5)	N3P2T1 to N3P2T10

Feed-forward distributed time delay	SSE	TRANSIG	5 to 50 (in a gap of 5)	N4P2T1 to N4P2T10
Generalized regression	SSE	TRANSIG	Spread constant 1 to 5	N5P2T1 to N5P2T5
Feed-forward backprop	MSE	PURELIN	5 to 50 (in a gap of 5)	N1P1P1 to N1P1P10
Cascade-forward backprop	MSE	PURELIN	5 to 50 (in a gap of 5)	N2P1P1 to N2P1P10
Elman-backprop	MSE	PURELIN	5 to 50 (in a gap of 5)	N3P1P1 to N3P1P10
Feed-forward distributed time delay	MSE	PURELIN	5 to 50 (in a gap of 5)	N4P1P1 to N4P1P10
Generalized regression	MSE	PURELIN	Spread constant 1 to 5	N5P1P1 to N5P1P5
Feed-forward backprop	SSE	PURELIN	5 to 50 (in a gap of 5)	N1P2P1 to N1P2P10
Cascade-forward backprop	SSE	PURELIN	5 to 50 (in a gap of 5)	N2P2P1 to N2P2P10
Elman-backprop	MSE	PURELIN	5 to 50 (in a gap of 5)	N3P2P1 to N3P2P10
Feed-forward distributed time delay	SSE	PURELIN	5 to 50 (in a gap of 5)	N4P2P1 to N4P2P10
Generalized regression	SSE	PURELIN	Spread constant 1 to 5	N5P2P1 to N5P2P5

Results and Discussion

The machining performance is evaluated in terms of cutting force, cutting temperature and surface roughness measured under each experimental condition. Comparative analysis is carried out across all thirteen cooling strategies and over the full range of cutting speed, feed and depth of cut, in order to quantify how lubrication mode and nanofluid formulation jointly influence the thermo-mechanical behaviour of the turning process.

Design of experiments run for all cooling condition cases

Design of Experiments (DOE) facilitates the study of operations because it provides a structured, statistical framework for varying multiple process factors simultaneously and measuring their impact on output, instead of changing one factor at a time. The steps followed for the Design of Experiments using RSM-based Box–Behnken Design (BBD) are illustrated in Figure *2*.

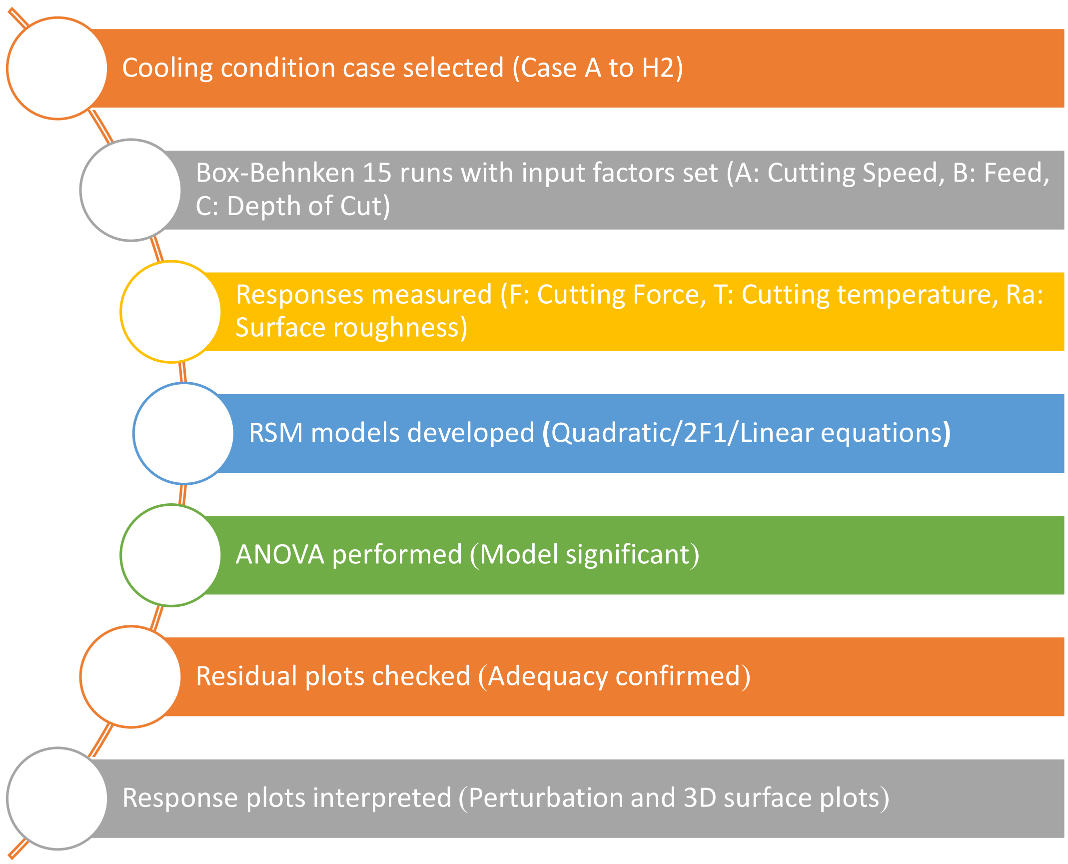

Figure 2 Steps followed for design of experiments using RSM based BBD

First, the specific cooling condition i.e. ***Case H1***, was selected and the corresponding 15-run Box–Behnken design was executed with cutting speed (A), feed (B) and depth of cut (C) as input factors. For every run, cutting force (F), cutting temperature (T) and surface roughness (Ra) were measured and compiled into the design matrix as given in Table 5. These data were then used to develop RSM models- linear for cutting force and cutting temperature, quadratic for surface roughness, as appropriate. Insignificant terms in the initial RSM model were systematically identified from ANOVA results and removed, thereby simplifying the regression equation without sacrificing predictive capability. Eliminating these statistically meaningless interaction or higher-order terms reduces overfitting and improves the numerical stability of the coefficients, allowing the final model to represent the true response surface more clearly over the design space.

Table 5 Box Behnken 15 runs for Case H1

Test Run	**Factor 1**	**Factor 2**	**Factor 3**	**Response 1**	**Response 2**	**Response 3**
	A: Cutting Speed	**B: Feed**	**C: DoC**	**Cutting Force**	**Cutting Temperature**	**Surface Roughness**
	m/min	**mm/rev**	**mm**	**N**	**°C**	**µm**
1	31.71	0.11	0.40	201.04	55.14	2.459
2	69.63	0.18	0.40	343.25	72.33	2.536
3	31.71	0.18	0.20	142.20	45.33	3.437

4	69.63	0.11	0.60	374.33	92.76	1.600
5	31.71	0.18	0.60	467.50	90.26	2.760
6	69.63	0.18	0.40	329.22	73.00	2.567
7	107.55	0.25	0.40	393.95	86.31	3.082
8	69.63	0.25	0.60	590.09	109.55	3.157
9	107.55	0.18	0.20	137.30	59.00	2.900
10	69.63	0.18	0.40	348.15	74.00	2.506
11	69.63	0.25	0.20	228.50	52.33	3.900
12	69.63	0.11	0.20	63.75	47.33	2.850
13	107.55	0.11	0.40	222.62	72.33	2.000
14	31.71	0.25	0.40	408.66	76.72	4.020
15	107.55	0.18	0.60	536.54	106.00	1.721

For Response 1, Cutting Force (F):

The software identifies a linear model (Table 6) as the most appropriate fit for the data. This model demonstrates high statistical significance, as evidenced by a p-value < 0.05.

Table 6 Fit summary for cutting force

Source	Sequential p-value	Lack of Fit p-value	Adjusted R²	Predicted R²	
Linear	**< 0.0001**	**0.1519**	**0.9788**	**0.9690**	**Suggested**
2FI	0.1825	0.1797	0.9836	0.9698	
Quadratic	0.0985	0.2898	0.9918	0.9612	
Cubic	0.2898		0.9958		**Aliased**

From Table 7, ANOVA for cutting force indicates that, due to the linear nature of the model, feed, and depth of cut are highly significant. The final regression model's actual equation for cutting force is given in Eq. (1).

Table 7 ANOVA table for cutting force

Source	Sum of Squares	Mean Square	F-value	p-value	
Model	315900	158000	316.09	< 0.0001	significant
B-Feed	72096.31	72096.31	144.26	< 0.0001	
C-DoC	243900	243900	487.93	< 0.0001	
Residual	5997.21	499.77			
Lack of Fit	5804.22	580.42	6.02	0.1509	not significant
Pure Error	192.99	96.49			
Cor Total	321900				

$$Cutting\ force\ (F) = 319.14 + 94.93 \times B + 174.59 \times C \quad (1)$$

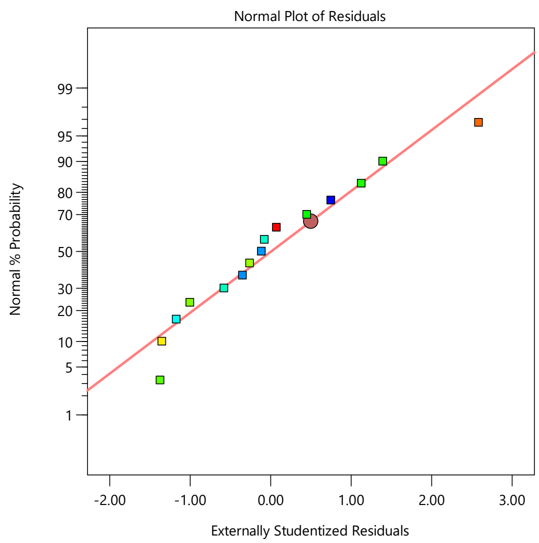

Figure 3 Normal probability plot of residuals for cutting force

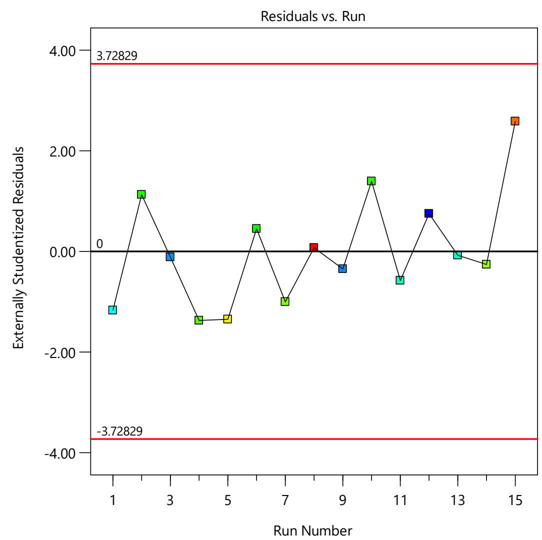

Figure 4 Externally studentized residuals vs run of experiments plot for cutting force

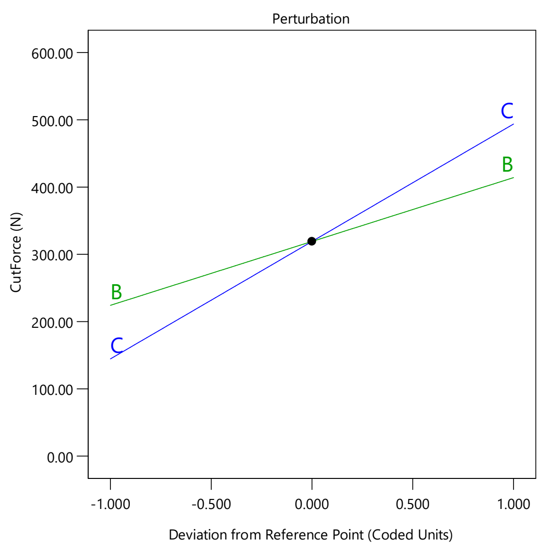

Figure 5 Perturbation plot for cutting force

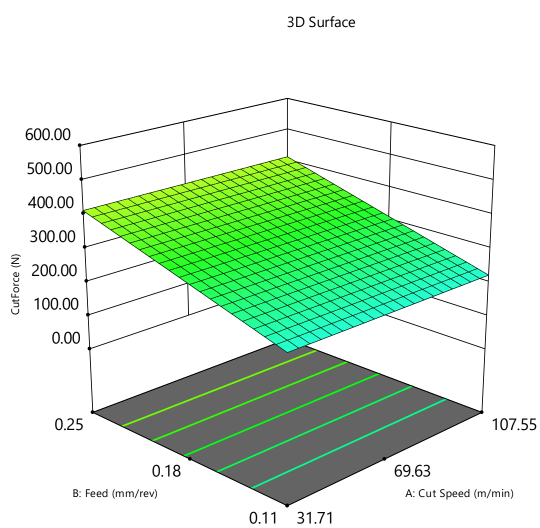

Figure 6 3D response surface plot showing the effect of cutting speed and feed on cutting force

The normal probability plot for cutting force is shown in Figure 3 and indicates that the residuals are close to the straight line. The terminology mentioned in the model is significant [16]. The externally studentized residuals versus run plot in Figure 4, indicates a point variation -3.72829 to 3.72829 range. It means this fitted model is suitable for the cutting force response. Regarding Figure 5 the effects of the input variables in perturbation plot are presented. It is noted that the cutting force increases proportionally with higher feed rates and depth of cut. The 3D response surface plot of cutting speed and feed is shown in Figure 6. From it, the minimum cutting force is at a cutting speed of 69.33 m/min, feed of 0.11 mm/rev and 0.2 mm DoC. It can also be seen that the maximum amount of cutting force happens at 69.33 m/min, feed of 0.25 mm/rev and 0.6 mm DoC.

For Response 2, Cutting Temperature (T):

The software identifies a linear model (Table 8) as the most appropriate fit for the data. This model demonstrates high statistical significance, as evidenced by a p-value < 0.05.

Table 8 Fit summary for cutting temperature

Source	Sequential p-value	Lack of Fit p-value	Adjusted R^2	Predicted R^2	
Linear	**< 0.0001**	**0.0542**	**0.9743**	**0.9575**	**Suggested**
2FI	0.1795	0.0645	0.9802	0.9431	
Quadratic	0.4716	0.0519	0.9800	0.8893	
Cubic	0.0519		0.9983		**Aliased**

From Table 9, ANOVA for cutting temperature indicates that, due to the linear nature of the model, cutting speed, feed, and depth of cut are highly significant. The final regression model's actual equation for cutting temperature is given in Eq. (2).

Table 9 ANOVA table for cutting temperature

Source	Sum of Squares	Mean Square	F-value	p-value	
Model	5537.93	1845.98	177.60	< 0.0001	significant
A-Cut Speed	394.66	394.66	37.97	< 0.0001	
B-Feed	411.08	411.08	39.55	< 0.0001	
C-DOC	4732.19	4732.19	455.28	< 0.0001	
Residual	114.33	10.39			
Lack of Fit	112.93	12.55	17.83	0.0542	not significant
Pure Error	1.41	0.7037			
Cor Total	5652.26				

$$Cutting\ temperature\ (T) = 74.16 + 7.02 \times A + 7.17 \times B + 24.32 \times C \quad (2)$$

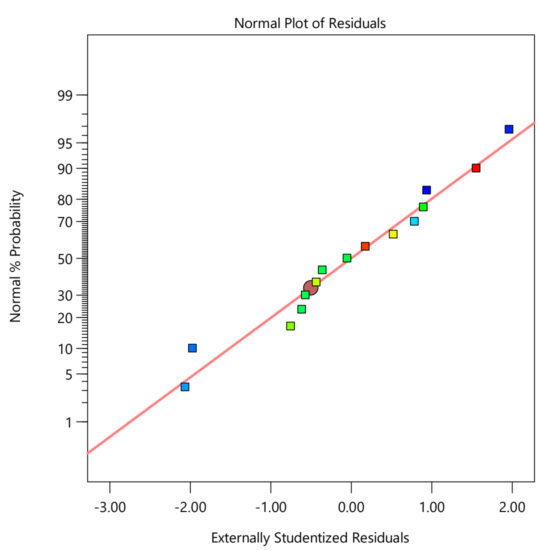

Figure 7 Normal probability plot of residuals for cutting temperature

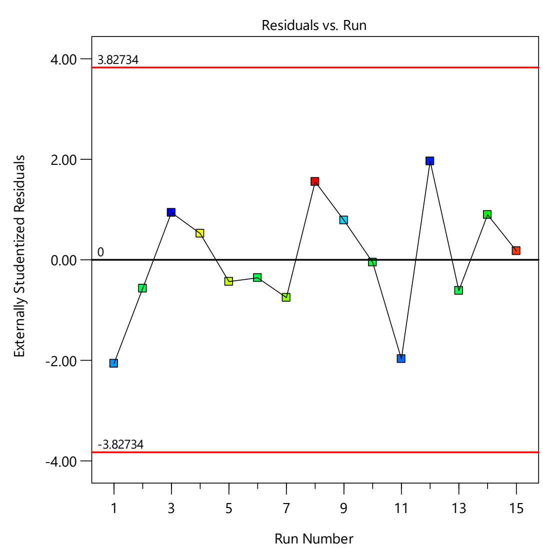

Figure 8 Externally studentized residuals vs run of experiments plot for cutting temperature

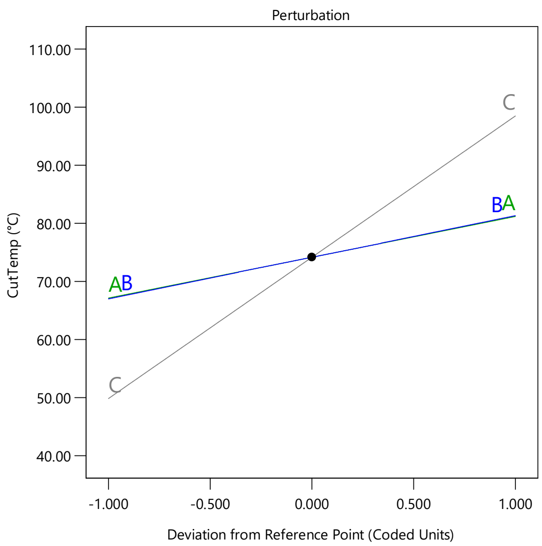

Figure 9 Perturbation plot for cutting temperature

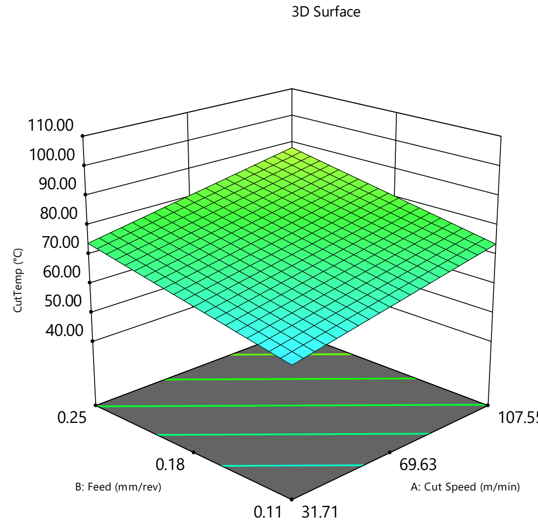

Figure 10 3D response surface plot showing the effect of cutting speed and feed on cutting force

The normal probability plot for cutting temperature is shown in Figure 7 and indicates that the residuals are close to the straight line. The terminology mentioned in the model is significant [16]. The externally studentized residuals versus run plot in Figure 8, indicates a point variation -3.82734 to 3.82734 range. It means this fitted model is suitable for the cutting temperature response. Regarding Figure 9 the effects of the input variables in perturbation plot are presented. It is noted that the cutting temperature increases proportionally with depth of cut. Also, it slightly increases with increase in both cutting speed and feed. The 3D response surface plot of cutting speed and feed is shown in Figure 10. From it, the minimum cutting temperature is at a cutting speed of 31.71 m/min, 0.18 mm/rev and 0.2 mm DoC. It can also be seen that the maximum amount of cutting temperature happens at 69.63 m/min, 0.25 mm/rev and 0.6 mm DoC.

For Response 3, Surface Roughness (Ra):

The software identifies a linear model (Table 10) as the most appropriate fit for the data. This model demonstrates high statistical significance, as evidenced by a p-value < 0.05.

Table 10 Fit summary for surface roughness

Source	Sequential p-value	Lack of Fit p-value	Adjusted R^2	Predicted R^2	
Linear	< 0.0001	0.0174	0.9116	0.8746	
2FI	0.2475	0.0189	0.9255	0.8709	
Quadratic	**0.0003**	**0.3131**	**0.9966**	**0.9842**	**Suggested**
Cubic	0.3131		0.9981		**Aliased**

From Table 11, ANOVA for surface roughness indicates that, due to the linear nature of the model, cutting speed, feed, and depth of cut are highly significant. The final regression model's actual equation for surface roughness is given in Eq. (3).

Table 11 ANOVA table for surface roughness

Source	Sum of Squares	Mean Square	F-value	p-value	
Model	6.87	0.7633	454.40	< 0.0001	significant
A-Cut Speed	1.10	1.10	657.24	< 0.0001	
B-Feed	3.45	3.45	2050.92	< 0.0001	
C-DOC	1.85	1.85	1102.17	< 0.0001	
AB	0.0574	0.0574	34.19	0.0021	
AC	0.0630	0.0630	37.50	0.0017	
BC	0.0642	0.0642	38.20	0.0016	
A²	0.0306	0.0306	18.20	0.0080	
B²	0.2557	0.2557	152.22	< 0.0001	
C²	0.0222	0.0222	13.20	0.0150	
Residual	0.0084	0.0017			
Lack of Fit	0.0065	0.0022	2.34	0.3131	not significant
Pure Error	0.0019	0.0009			
Cor Total	6.88				

$$\begin{aligned} Surface\ roughness\ (Ra) \\ &= 2.54 - 0.3715 \times A + 0.6562 \times B - 0.4811 \times C - 0.1198 \times A \times B \\ &- 0.1255 \times A \times C + 0.1267 \times B \times C + 0.0910 \times A^2 + 0.2632 \times B^2 \\ &+ 0.0775 \times C^2 \end{aligned} \quad (3)$$

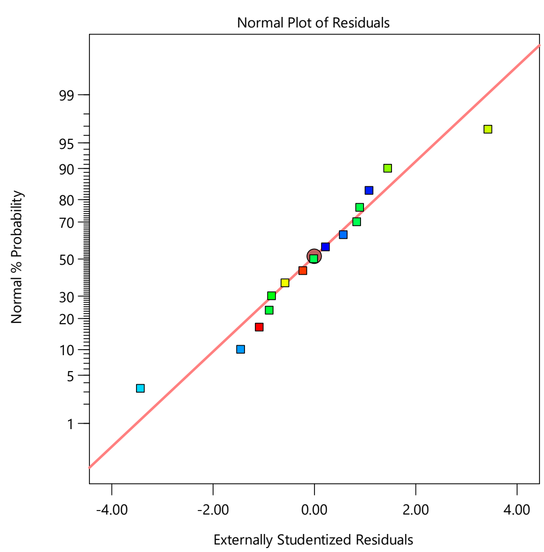

Figure 11 Normal probability plot of residuals for surface roughness

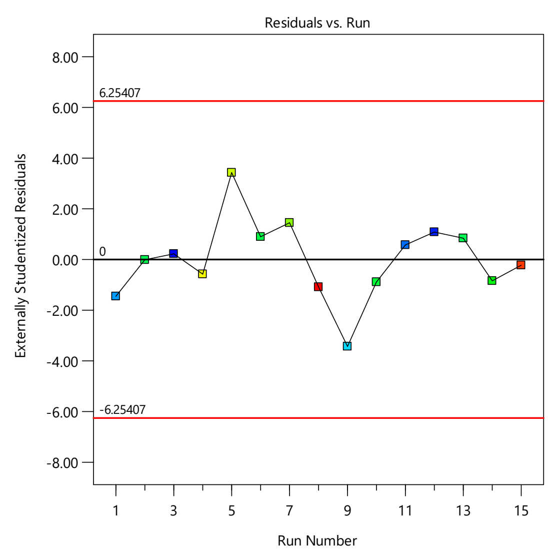

Figure 12 Externally studentized residuals vs run of experiments plot for surface roughness

The normal probability plot for surface roughness is shown in Figure 11 and indicates that the residuals are close to the straight line. The terminology mentioned in the model is significant [16]. The externally studentized residuals versus run plot in Figure 12, indicates a point variation -6.25407 to 6.25407 range. It means this fitted model is suitable for the surface roughness response. Regarding Figure 13 the effects of the input variables in perturbation plot are presented. It is noted that the surface roughness increases with increase in feed. Furthermore, it decreases with increase in cutting speed and depth of cut.

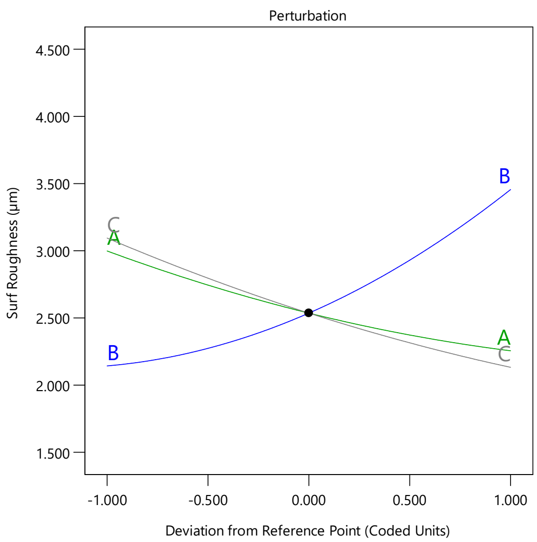

Figure 13 Perturbation plot for surface roughness

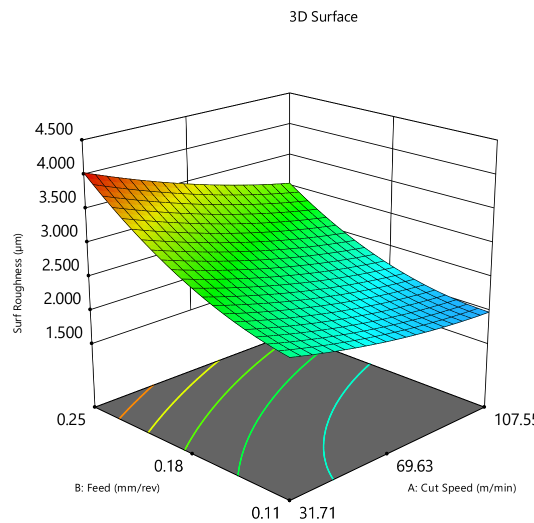

Figure 14 3D response surface plot showing the effect of cutting speed and feed on surface roughness

The 3D response surface plot of cutting speed and feed is shown in Figure 14. From it, the minimum surface roughness is at a cutting speed of 69.63 m/min, 0.11 mm/rev and 0.6 mm DoC. It can also be seen that the maximum amount of surface roughness happens at 31.71 m/min, 0.25 mm/rev and 0.4 mm DoC.

For Case H1, the RSM models for cutting force, temperature, and surface roughness all show (Table 12) excellent adequacy, with R^2, adjusted R^2, and predicted R^2 generally above 0.95, indicating that they explain almost all variability in the data and predict new points reliably within the design space [17].

Table 12 Model adequacy metrics for Case H1 output responses

Type	Cutting Force	Cutting Temperature	Surface Roughness
R^2	0.9833	0.9798	0.9988
Adjusted R^2	0.9788	0.9743	0.9966
Predicted R^2	0.9690	0.9575	0.9842

The same RSM-based Box–Behnken design and analysis procedure was applied independently to all thirteen cooling condition cases (A–H2), and outcomes are discussed as follows:

RSM analysis of the Box–Behnken design showed that surface roughness increases markedly with feed, while lower cutting speed and smaller depth of cut favour improved surface finish. Across all responses, ANOVA results indicated that factors with p-values below 0.05 have a statistically significant effect, with large F-values confirming the strong influence of feed and depth of cut, while model-adequacy metrics (R^2 typically above 0.95, high adjusted and predicted R^2) and well-behaved residual, perturbation and 3D surface plots verified that the developed models accurately represent the response surfaces throughout the design space.

Comparison of cooling strategies revealed that dry cutting (Case A) produces the highest temperatures and poorest surface finish, wet cooling with conventional fluids (Cases B, C) substantially decreases temperature but does not consistently minimise Ra, and MQL with mono nanofluids (Al_2O_3 or ZnO, Cases D1-E2) further improves cooling and often reduces forces, with generally better surface quality than dry and competitive performance relative to wet cutting. Among all conditions, MQL with hybrid Al_2O_3-ZnO nanofluids (Cases F1–H2) provided the most balanced behaviour, combining forces comparable to or better than wet cutting with much lower temperatures than dry and significantly reduced roughness. The physics of the nanofluid lubrication explain these outcomes: Al_2O_3 - rich fluids form a hard, load-bearing tribofilm and promote micro-rolling/polishing at the tool-chip interface, giving superior reductions in cutting force and Ra, whereas ZnO-rich fluids contribute more to heat removal due to their higher thermal conductivity, particularly at elevated speeds; at about 1 wt% total nanoparticles the combined effects on thermal conductivity and tribofilm formation are strongest without excessive viscosity or agglomeration, leading to the best overall cooling case performance.

Comparison of all cooling condition

The overall performance across the thirteen cooling conditions was compared using a multi-response "smaller-is-better" desirability index d [18], as per Eq. (4), constructed from the output response value in each case, with the overall desirability D [Eq. (5)], taken as the geometric mean of the three single-response desirability.

$$d = \frac{Y_{max} - Y}{Y_{max} - Y_{min}} \tag{4}$$

where Y_{max} and Y_{min} are the worst and best values across all 13 cases for that response.

$$D = \left(d_{F,} d_{T,} d_{Ra}\right)^{1/3} \tag{5}$$

The resulting ranking shown in Table 13 that MQL with 1 wt% Al_2O_3:ZnO (75:25, Case H1) is the best condition, combining the globally lowest surface roughness (1.6 µm) with simultaneously low force and temperature; dry cutting (Case A) appears second mainly because its best-case force and Ra are numerically low despite high temperature and poor sustainability. Among the nanofluid MQL cases, the next strongest multi-response performers after H1 are G2 (2 wt% Al_2O_3:ZnO , 50:50) and E1 (1 wt% ZnO), which provide a reasonable compromise between force, temperature and roughness, whereas conventional wet cases B and C rank lower due to relatively poor surface finish even though they achieve low temperatures.

Table 13 Ranked multi-response performance (global minima basis)

Rank	Cooling Condition Case	Global-min F (N)	Global-min T (°C)	Global-min Ra (µm)	Overall D
1	Case-H1 [MQL + 1% wt (Al_2O_3 : ZnO, 75:25)])	63.75	45.33	1.6	0.621
2	Case-A Dry	63.75	48.84	1.75	0.472

3	Case-G2 [MQL + 2% wt (Al_2O_3 : ZnO, 50:50)]	83.36	45.4	2.341	0.468
4	Case-E1 MQL + 1% wt ZnO	88.26	46.67	2.02	0.45
5	Case-D1 MQL + 1% wt Al_2O_3	62.08	49	2.252	0.423
6	Case-D2 MQL + 2% wt Al_2O_3	102.97	47.89	2.097	0.342
7	Case-H2 [MQL + 2% wt (Al_2O_3 : ZnO, 75:25)]	104.64	40.66	3.15	0.321
8	Case-E2 MQL + 2% wt ZnO	83.36	50.33	2.05	0.317
9	Case-C Wet SAE40	67.86	51.67	1.678	0.22
10	Case-G1 [MQL + 1% wt (Al_2O_3 : ZnO, 50:50)]	98.07	42	3.645	0.102
11	Case-B Wet Conventional Fluid	42.46	31.33	3.659	very low

Multi-objective optimization and validation

For selected Case H1, the multi-objective optimization [19], [20] was performed using a desirability function approach (DFA) [21], [22] based on the Box–Behnken RSM models for cutting force, cutting temperature and surface roughness, with "lower is better" as the goal for all three responses. Surface roughness is given the highest weight (0.5), followed by cutting force (0.3) and temperature (0.2), leading to the choice of a high cutting speed with low feed and low depth of cut; physically, higher speed improves finish but raises temperature, higher feed strongly increases both force and Ra, and higher depth of cut increases force and often temperature and roughness [20], [23], so the selected optimum inputs are A = 107.55 m/min, B = 0.11 mm/rev and C = 0.2 mm. Within the specified bounds for each factor and response (Table 14), 34 available solutions are evaluated and the one with maximum overall desirability (D = 0.943) is selected, corresponding to predicted responses of about 49.6 N cutting force, 49.7 °C cutting temperature and 2.79 µm surface roughness at this optimum parameter combination. For optimum condition, value of output predicted response for optimum inputs has been shown in contour plot in Figure 15.

Table 14 Criteria table for optimum condition

Parameter	Goal	Lower Limit	Upper Limit	Weight
A: Cutting Speed	maximize	31.71	107.55	1
B: Feed	minimize	0.11	0.25	1
C: Depth of Cut	minimize	0.2	0.6	1
F: Cutting Force	minimize	63.75	590.08	0.3
T: Cutting Temperature	minimize	45.33	109.55	0.2
Ra: Surface Roughness	minimize	1.6	4.02	0.5

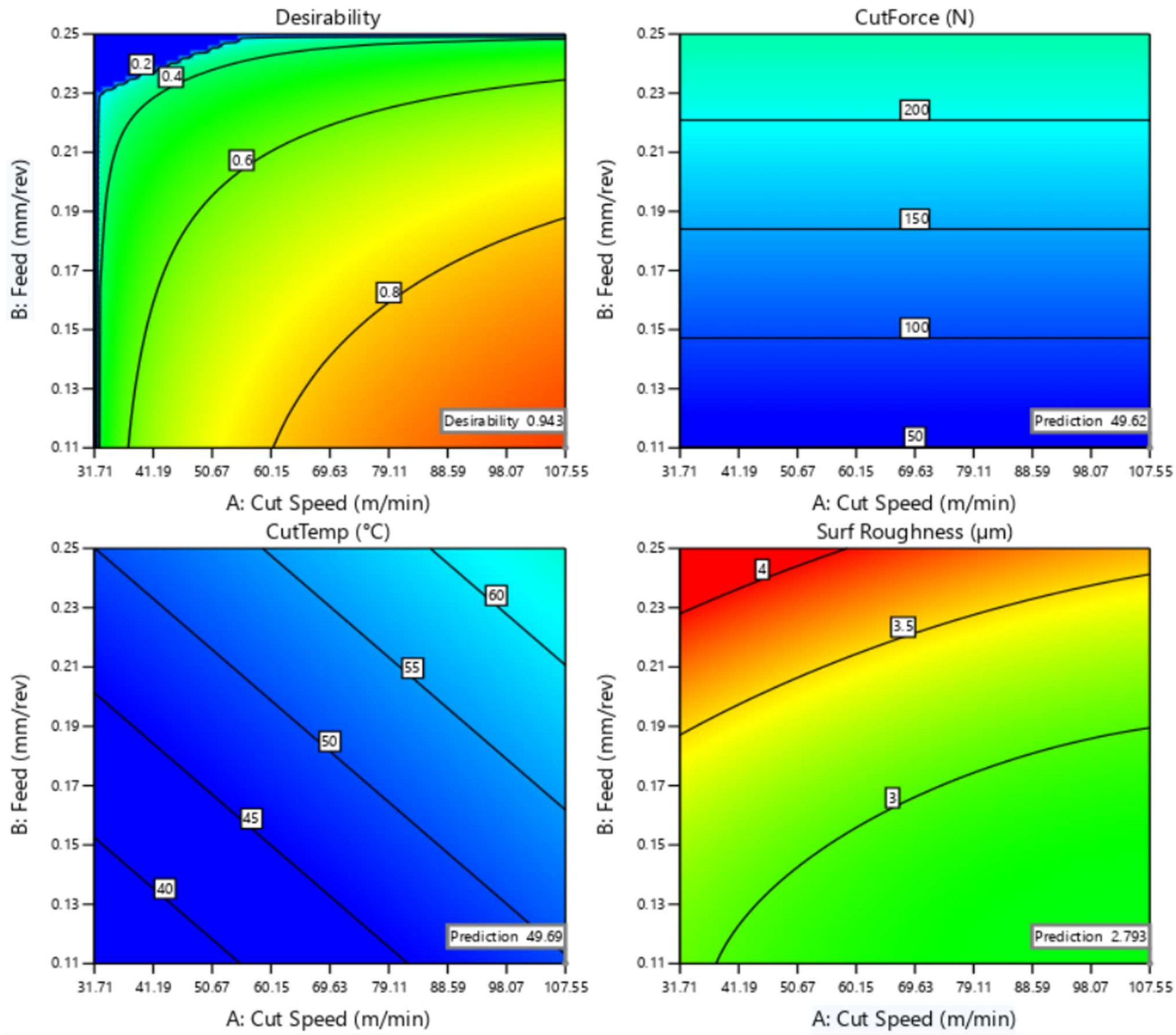

Figure 15 Contour plot for optimum condition with predicted output value

Once the optimal parameter values were identified, the final task is to validate the predicted outputs by performing a validation experiment. The aim of the validating experiment is to verify conclusions derived in the statistical analysis stage and the improvement of measured output performance using the optimum level. For Case H1 as a cooling method, the optimum condition, with a high desirability value of 0.943, for Cutting Force, Cutting Temperature, and Surface Roughness is as follows: A = 107.55 m/min, B = 0.11 mm/rev, and C = 0.2 mm.

Table 15 indicates that experimentation runs extracts the expected and actual answers and compares them with the predicted value. The percentage errors between experimental means and RSM predictions were 8.23% (cutting force), 6.83% (temperature), and 3.56% (surface roughness). The percentage errors between the predicted and mean experimental values are with acceptable accuracy. It is confirming the high predictive accuracy of the developed RSM models.

Table 15 Combination of optimum parameters for confirmation experimentation run for Case H1

Output Parameter	Predicted value by RSM	Mean experiment value	Percentage error (%)
Cutting Force	49.62	54.07	8.23
Cutting Temperature	49.69	53.33	6.83
Surface Roughness	2.793	2.896	3.56

ANN model for predicting the performance of cooling condition

Several network architectures were investigated, including feed-forward backpropagation, cascade-forward, Elman and distributed time-delay networks, as well as generalized regression neural networks, by systematically varying performance functions (MSE and SSE), transfer functions (TRANSIG and PURELIN) and the number of neurons in the hidden layer (5–50 in steps of 5, or spread constants for GRNN), resulting in 190 trained and simulated networks. The prediction capability of each configuration was assessed using mean squared error (MSE), normalized MSE (NMSE), mean absolute error (MAE), mean absolute relative deviation (MARD), mean relative error (MRE), average actual error (AAE), mean absolute percentage error (MAPE) and the coefficient of determination R^2, and the final ANN model was selected based on the combination of the lowest error indices and the highest R^2, ensuring reliable generalization for cooling-condition performance prediction.

The best ANN model by including all experimental cases is N4P2T2, a single layer feed-forward distributed delay network with 10 neurons in the hidden layer and TRANSIG transfer function.

Achievements with respect to objectives

Objectives	Achievements
To experimentally investigate the effects of cutting speed, feed and depth of cut on turning performance under different cooling strategies (dry, wet, simple MQL, MQL with mono nanofluid and MQL with hybrid nanofluid).	Systematic turning experiments were conducted under dry, wet, simple MQL, MQL with mono nanofluid and MQL with hybrid nanofluid, with same cutting speed, feed and depth of cut as an input parameter; this enabled quantification of how each cooling strategy influences cutting temperature, cutting force and surface roughness. (Attained with experimental evaluation of cooling strategies)
To compare dry, wet, MQL+wet, MQL+mono nanofluid and MQL+hybrid nanofluid conditions in	The measured responses clearly showed that nanofluid-assisted MQL, particularly with hybrid nanofluids, outperformed dry, wet, and simple MQL

terms of cutting temperature, cutting force and surface roughness.	conditions, yielding lower cutting temperatures, reduced cutting forces and improved surface finish; these differences were statistically confirmed through ANOVA. (Attained with comparative performance analysis)
To determine the optimum cutting-fluid strategy and operating parameters for MQL-assisted turning, using multi-response optimization based on the measured performance indicators.	Multi-response optimization (using desirability function approach) was applied to the experimental data to determine the best combination of cutting speed, feed, depth of cut and nanofluid type, thereby identifying an optimum MQL-based cooling configuration for turning. (MQL with 1 wt% hybrid Al_2O_3:ZnO (75:25, Case H1) with 107.55 m/min cutting speed, 0.11 mm/rev feed, and 0.2 mm depth of cut as the optimum cutting-fluid strategy)
To develop and train Artificial Neural Network (ANN) models and identify the most accurate ANN architecture for predicting turning performance under different cooling conditions.	Several ANN architectures were developed and trained using the experimental dataset, and their predictive capabilities for cutting force, temperature and surface roughness under different cooling conditions were compared; the selected ANN model achieved high coefficients of determination (R^2) and low prediction error, demonstrating reliable performance prediction for cooling condition. (The best ANN model has been suggested)

Conclusion

Understanding the fundamentals of heat transfer is crucial for designing mono and hybrid nanofluids for advanced cooling and lubrication, particularly in machining applications. In the present work, experimental and ANN-based investigations were carried out on AISI 1040 turning under thirteen cooling strategies, ranging from dry and wet cutting to MQL with Al_2O_3, ZnO and Al_2O_3-ZnO hybrid nanofluids, where RSM-based Box–Behnken models and multi-response desirability optimization were used to quantify and optimize cutting force, cutting temperature and surface roughness, and an ANN model was subsequently developed and selected based on minimum prediction error and high R^2 for reliable prediction of cooling-condition performance.

1. The RSM-based Box–Behnken designs were applied independently to all thirteen cooling conditions (Cases A-H2), and ANOVA confirmed that the models for cutting force, cutting temperature and surface roughness are statistically significant in every case. The models exhibit high R^2 and adjusted R^2 (typically above 0.95) with acceptable predicted R^2, normal probability

and residual–predicted plots show no serious violations of normality or constant variance, and perturbation and response-surface plots closely follow experimental trends, demonstrating that the RSM models are adequate and reliable.

2. Feed and depth of cut are identified as the main contributors to increased cutting force, cutting temperature and surface roughness, whereas cutting speed has a moderate but significant and more complex influence. Higher feed markedly increases chip thickness, leading to large rises in force, temperature and roughness, while higher depth of cut mainly amplifies cutting force via larger chip cross-section and contact length and also tends to increase temperature and roughness; cutting speed tends to improve Ra at moderate levels by reducing built-up edge but raises temperature and slightly lowers force due to thermal softening.

3. Selection between Al_2O_3 and ZnO nanofluids can be made on the basis that Al_2O_3 is preferable for surface integrity and lower forces, while ZnO is more effective for thermal management at high speed. Al_2O_3 nanofluid yields consistently lower surface roughness and cutting force due to its tribological behaviour (formation of a load-bearing tribofilm and micro-rolling/polishing effect), whereas ZnO-based nanofluids reduce cutting temperature more strongly thanks to higher thermal conductivity; an intermediate concentration around 1 wt% gives the best overall performance, while higher loadings (1.5–2 wt%) increase viscosity and agglomeration, degrading lubrication.

4. A multi-response desirability index with equal weighting of cutting force, cutting temperature and surface roughness (smaller-is-better) ranks MQL with 1 wt% hybrid Al_2O_3-ZnO (75:25, Case H1) as the most suitable lubrication condition among the thirteen cases. Case H1 provides the globally lowest surface roughness (about 1.6 μm) together with moderately low force and temperature compared with both mono-nanofluid and conventional conditions, demonstrating a clear synergistic effect between Al_2O_3 and ZnO nanoparticles on mechanical (force, Ra) and thermal (temperature) performance.

5. Desirability Function Analysis coupled with RSM identified the optimal cutting parameters for Case H1 as cutting speed 107.55 m/min, feed 0.11 mm/rev and depth of cut 0.2 mm. Confirmation experiments at this setting showed low prediction errors (about 8.23% for cutting force, 6.83% for cutting temperature and 3.56% for surface roughness), confirming that the developed RSM models and DFA-based optimization provide accurate and practically useful predictions.

6. At the same optimum input condition, Case H1 (hybrid nanofluid MQL) achieves reductions of approximately 25.1%, 18.26% and 16.33% in cutting force, cutting temperature and surface

roughness, respectively, when compared with dry cutting (Case A).

7. Among all ANN architectures evaluated, the best-performing model for predicting cooling-condition performance is the N4P2T2 configuration, i.e., a feed-forward distributed time-delay network with TANSIG transfer function and 10 neurons in the hidden layer.

Future research may extend the present work by exploring wider ranges of cutting parameters, different tool geometries and wear conditions, and hard-to-machine alloys and coated tools, as well as by generalizing the methodology to other machining operations such as milling, drilling and grinding. In parallel, nanofluid formulations can be further optimized by varying nanoparticle concentration, employing alternative base oils and developing more complex systems such as tri-hybrid nanoparticle mixtures to enhance stability, cooling and lubrication performance. Finally, integrating advanced optimization schemes and AI-based predictive models with comprehensive sustainability, economic and health-impact assessments would support the industrial-scale implementation of hybrid nanofluid MQL as a practical, green machining technology.

LIST OF ALL PUBLICATIONS

1. **A. H. Nalbandh**, N. K. Chavda, and R. K. Bumataria, "Response Surface Methodology-based Modeling and Optimization of AISI 1040 Turning Using Al_2O_3 and ZnO Nanofluids Under Minimum Quantity Lubrication," *Journal of Environmental Nanotechnology*, vol. 15(1), March, pp. 603–615, 2026. https://doi.org/10.13074/jent.2026.03.2612063 **(Scopus)**

2. **A. H. Nalbandh**, N. K. Chavda, and R. K. Bumataria, "Comparative Study of Mono and Hybrid Nanofluids in MQL Turning of AISI 1040 Steel Using Box–Behnken RSM Approach," *International Journal of Technology & Emerging Research*, vol. 2(4), April, pp. 26–44, 2026. https://doi.org/10.64823/ijter.2604004 **(Academia)**

3. **A. H. Nalbandh**, N. K. Chavda, and R. K. Bumataria, "Current research aspects in minimum quantity lubrication for turning operations: Cutting fluid as mono and hybrid nanofluid," *Sigma Journal of Engineering and Natural Science*, vol. 44(2), April, pp. 1344–1368, 2026. https://doi.org/10.14744/sigma.2026.2041 **(ESCI, Scopus)**

4. **A. H. Nalbandh**, N. K. Chavda, and R. K. Bumataria, "Performance Analysis of AISI 1040 Steel Turning Under Al_2O_3–ZnO Hybrid Nanofluid MQL Using Response Surface Methodology - A Step Towards Sustainable Machining," *Journal of Materials and Engineering*, vol. 4(2), pp. 155–168. https://jme.aspur.rs/archive/v4/n2/3.php **(Article in Press, Pre-print)**

PATENTS

1. **Nalbandh, A. H.,** Chavda N. K., Bumataria, R. K. Nandaniya M. P., GTU, A System and Method for Minimum Quantity Lubrication Incorporating a Dual-Nanoparticle Cutting Fluid Composition and its Synthesis for Turning Operations, Patent journal: 27/2025 dated: 04/07/2025, No.202521056040A.

REFERENCES

[1] A. J. P, A. Xavior, and R. Scholar, "'Influence Of Nano Lubrication In Machining Operations-A Review,'" *Mater. Today Proc.*, vol. 5, pp. 11185–11192, 2018, doi: 10.1016/j.matpr.2018.01.142.

[2] V. S. Sharma, G. Singh, and K. Sorby, "A review on minimum quantity lubrication for machining processes," *Materials and Manufacturing Processes*, vol. 30, no. 8, pp. 935–953, Aug. 2015, doi: 10.1080/10426914.2014.994759.

[3] A. K. Sharma, A. K. Tiwari, and A. R. Dixit, "Effects of Minimum Quantity Lubrication (MQL) in machining processes using conventional and nanofluid based cutting fluids: A comprehensive review," Jul. 20, 2016, *Elsevier Ltd*. doi: 10.1016/j.jclepro.2016.03.146.

[4] N. Madanchi, D. Kurle, M. Winter, S. Thiede, and C. Herrmann, "Energy efficient process chain: The impact of cutting fluid strategies," *Procedia CIRP*, vol. 29, pp. 360–365, 2015, doi: 10.1016/j.procir.2015.02.056.

[5] L. V. Suryam, A. V. Pradeep, S. V. Satya Prasad, and P. Prasanna Kumari, "Functioning mechanism of nanomaterials and significance on machinability: A review," in *Materials Today: Proceedings*, Elsevier Ltd, 2019, pp. 560–563. doi: 10.1016/j.matpr.2019.07.733.

[6] R. K. Bumataria, N. K. Chavda, and H. Panchal, "Current research aspects in mono and hybrid nanofluid based heat pipe technologies," *Heliyon*, vol. 5, no. 5, p. e01627, 2019, doi: 10.1016/j.heliyon.2019.e01627.

[7] Z. Said *et al.*, "A comprehensive review on minimum quantity lubrication (MQL) in machining processes using nano-cutting fluids," *International Journal of Advanced Manufacturing Technology*, vol. 105, no. 5–6, pp. 2057–2086, Dec. 2019, doi: 10.1007/s00170-019-04382-x.

[8] A. NALBANDH, N. CHAVDA, and R. BUMATARIA, “Current research aspects in minimum quantity lubrication for turning operations: Cutting fluid as mono and hybrid nanofluid,” *Sigma Journal of Engineering and Natural Sciences – Sigma Mühendislik ve Fen Bilimleri Dergisi*, vol. 44, no. 2, pp. 1344–1368, Apr. 2026, doi: 10.14744/sigma.2026.2041.

[9] S. Haghnazari and V. Abedini, “Effects of hybrid Al2O3–CuO nanofluids on surface roughness and machining forces during turning AISI 4340,” *SN Appl. Sci.*, vol. 3, no. 2, Feb. 2021, doi: 10.1007/s42452-020-04088-w.

[10] R. A. Laghari, M. Jamil, A. A. Laghari, and A. M. Khan, “Material characteristics and machinability of metal matrix composite materials: A critical review on recent advances and future perspectives,” *Measurement*, vol. 242, p. 115839, Jan. 2025, doi: 10.1016/j.measurement.2024.115839.

[11] K. Apmann, R. Fulmer, A. Soto, and S. Vafaei, “Thermal Conductivity and Viscosity: Review and Optimization of Effects of Nanoparticles,” *Materials*, vol. 14, no. 5, p. 1291, Mar. 2021, doi: 10.3390/ma14051291.

[12] A. K. Sharma, R. K. Singh, A. R. Dixit, and A. K. Tiwari, “Characterization and experimental investigation of Al2O3 nanoparticle based cutting fluid in turning of AISI 1040 steel under minimum quantity lubrication (MQL),” *Mater. Today Proc.*, vol. 3, no. 6, pp. 1899–1906, 2016, doi: 10.1016/j.matpr.2016.04.090.

[13] O. Özbek, N. Altan Özbek, F. Kara, and H. Saruhan, “Effect of vibration and cutting zone temperature on surface topography during hybrid cooling/lubrication assisted machining of Vanadis 10,” *Materials Testing*, vol. 65, no. 9, pp. 1437–1452, Sep. 2023, doi: 10.1515/mt-2023-0057.

[14] F. Günan, T. Kıvak, Ç. V. Yıldırım, and M. Sarıkaya, “Performance evaluation of MQL with AL2O3 mixed nanofluids prepared at different concentrations in milling of Hastelloy C276 alloy,” *Journal of Materials Research and Technology*, vol. 9, no. 5, pp. 10386–10400, Sep. 2020, doi: 10.1016/j.jmrt.2020.07.018.

[15] Z. Said *et al.*, “Recent advances on the fundamental physical phenomena behind stability, dynamic motion, thermophysical properties, heat transport, applications, and challenges of nanofluids,” Feb. 02, 2022, *Elsevier B.V.* doi: 10.1016/j.physrep.2021.07.002.

[16] D. C. Montgomery, *Design and analysis of experiments*, 8th ed. Hoboken NJ: John Wiley & Sons, Inc., 2013.

[17] B. Öztürk, Ö. Küçük, M. Aydın, and F. Kara, "Machine Learning-Guided Energy-Efficient Machining of 8000 Series Aluminum Alloys," *Machines*, vol. 13, no. 10, p. 906, Oct. 2025, doi: 10.3390/machines13100906.

[18] Fethi Khelfaoui, M. A. Yallese, N. Ouelaa, S. Chihaoui, and S. Belhadi, "Statistical analysis, modeling and multi-objective optimization of parameters intermittent turning process of AISI D3," *Journal of Mechanical Engineering and Sciences*, pp. 9492–9506, Jun. 2023, doi: 10.15282/jmes.17.2.2023.8.0752.

[19] F. Kara, A. Takmaz, Ö. Erkan, and S. Filiz, "Response Surface Method Optimization of Hard Machining with Cryogenically Treated Cutting Tools: Surface Roughness, Cutting Force, Tool Wear, Rietveld Analysis, and Metallurgical Properties," *Steel Res. Int.*, vol. 96, no. 7, Jul. 2025, doi: 10.1002/srin.202400850.

[20] E. M. Gutema, M. Gopal, and H. G. Lemu, "Minimization of Surface Roughness and Temperature during Turning of Aluminum 6061 Using Response Surface Methodology and Desirability Function Analysis," *Materials*, vol. 15, no. 21, p. 7638, Oct. 2022, doi: 10.3390/ma15217638.

[21] R. V Prasad, R. Rajesh, D. Thirumalaikumarasamy, M. Ashokkumar, and S. Rajakumar, "Multi response optimization of HVOF process parameters in low carbon steels," *Sādhanā*, vol. 47, no. 4, p. 265, Dec. 2022, doi: 10.1007/s12046-022-02045-4.

[22] P. Kanti, K. V. Sharma, K. M. Yashawantha, and S. Dmk, "Experimental determination for viscosity of fly ash nanofluid and fly ash-Cu hybrid nanofluid:Prediction and optimization using artificial intelligent techniques," *Energy Sources, Part A: Recovery, Utilization, and Environmental Effects*, vol. 47, no. 2, Dec. 2025, doi: 10.1080/15567036.2021.1877374.

[23] A. Ercetin, K. Aslantaş, Ö. Özgün, M. Perçin, and M. P. G. Chandrashekarappa, "Optimization of Machining Parameters to Minimize Cutting Forces and Surface Roughness in Micro-Milling of Mg13Sn Alloy," *Micromachines (Basel).*, vol. 14, no. 8, p. 1590, Aug. 2023, doi: 10.3390/mi14081590.